JOURNAL OF BACTERIOLOGY, Mar. 1997, p. 1951–1961 Vol. 179, No. 6
0021-9193/97/$04.00+0

Evidence for the Role of Redox Carriers in Photosynthesis Gene Expression and Carotenoid Biosynthesis in *Rhodobacter sphaeroides* 2.4.1

JAMES P. O'GARA AND SAMUEL KAPLAN*

Department of Microbiology and Molecular Genetics, Medical School, The University of Texas Health Science Center, Houston, Texas 77030

Received 28 August 1996/Accepted 14 January 1997

Previous work from this laboratory revealed that alterations in the structure of the *ccoNOQP* operon of *Rhodobacter sphaeroides* 2.4.1 could lead to induction of the photosynthetic apparatus under aerobic growth conditions. Immediately downstream of the *ccoNOQP* operon is the *rdxB* gene, the first gene of the *rdxBHIS* cluster. The *rdxB* gene product is predicted to encode a membrane protein which can bind two [4Fe-4S] clusters. The *ccoP* gene product is a diheme cytochrome which is a component of the cbb_3-type cytochrome oxidase. Under aerobic growth conditions, strains possessing *ccoP* and *rdxB* mutations both singly and in combination produced light-harvesting complexes, suggesting that normal functioning of these proteins is required to maintain repression of photosynthesis gene expression in the presence of oxygen. Analysis of the expression of *puc*::*lacZ* fusions under aerobic conditions revealed an approximately 12-fold increase in *puc* operon expression in the RDXB1 and CCOP1 mutant strains compared with that for wild-type 2.4.1. Similarly, *puf*::*lacZ* activity was observed to be elevated fourfold above wild-type levels. Further indication of the importance of the RdxB and CcoP proteins was derived from studies of mutant and wild-type cells grown under anoxygenic photosynthetic and nitrogen-fixing conditions. These mutant strains were observed to accumulate spheroidenone to approximately 50% or more of the total carotenoid. In wild-type cultures, spheroidenone normally accumulates to approximately 10 to 20% of the total carotenoid under the same growth conditions. This effect was most pronounced when both the *rdxB* and the *ccoP* mutations were present together in cells cultured under nitrogen-fixing photosynthetic growth conditions in which spheroidenone represented approximately 90% of the total carotenoid. We propose that mutations in the *rdxB* or *ccoP* gene may lead to changes in a membrane-generated redox signal or the accumulation of a critical redox intermediate in the mutant strains which results in increased photosynthesis gene expression under aerobic conditions by alteration of the activity of a transcriptional regulator(s) of photosynthesis gene expression. Mutations in these genes also appear to posttranscriptionally influence the terminal step of carotenoid biogenesis. Potential regulators interacting with an aberrant redox signal in the mutants and the possible nature of such a redox signal are discussed.

The remarkable metabolic versatility of *Rhodobacter sphaeroides* permits its survival and growth in a wide range of ecosystems by employing a variety of growth modes including aerobic, photosynthetic, and diazotrophic modes and anaerobic growth in the dark. Under low-oxygen tensions, *R. sphaeroides* synthesizes two photosynthetic light-harvesting complexes, B800-850 or LHII and B875 or LHI, which trap light energy and transfer exciton energy to the reaction center. The light-harvesting complexes are part of the intracytoplasmic membrane (ICM) of photoheterotrophically growing cultures and are comprised of integral membrane-localized structural polypeptides associated with the photopigments bacteriochlorophyll (Bchl) and carotenoids (Crt) (reviewed in reference 16). The Crt content of *R. sphaeroides* is primarily composed of spheroidene (SE) and spheroidenone (SO) (32). However, the relative abundance of SE, a yellow carotenoid, and SO, a red carotenoid, is dependent on the growth mode of the cells. In aerobic and semiaerobic cultures, SO is predominant, although the overall Crt content is low, whereas under photosynthetic and anaerobic conditions SE is the major carotenoid and the total Crt content is high (3, 32, 34). The end product of the Crt pathway, SO, is synthesized via the oxidation of SE in a reaction catalyzed by the *crtA* gene product (1, 17) which has never been demonstrated in vitro. Recently, it has been demonstrated that SE is associated principally with the B800-850 LH complex, while SO is the more abundant Crt in the B875 antenna complex and that the relative accumulations of SE and SO may affect the formation of the two antenna complexes (39). It was further shown that the conversion of SE to SO was affected by a number of environmental parameters, e.g., O_2, light, and external electron acceptors, all of which have in common their likely effect on cellular redox poise (39).

Syntheses of Bchl, Crt, and the structural polypeptides of the B875 and B800-850 complexes are all regulated in response to both oxygen and light (16). Understanding the ability of *R. sphaeroides* to sense and respond to changes in oxygen tension has been the focus of numerous studies, and, to date, four discrete aerobic-anaerobic response regulatory systems have been identified (6, 7, 10, 40, 42).

It was further documented that alterations in the structure of the *ccoNOQP* operon encoding the cbb_3-type terminal oxidase, which has been purified from *R. sphaeroides* (8), could result in the accumulation of the ICM in the presence of O_2 (43). Immediately downstream of *ccoNOQP* is the *rdxB* gene, a homolog of *rdxA* (42). We use the term homolog to define pairs of genes, each mapping to a separate *R. sphaeroides*

* Corresponding author. Phone: (713) 794-1742. Fax: (713) 794-1782. E-mail: microbiology@utmmg.med.uth.tmc.edu.

TABLE 1. Strains and plasmids

Strain or plasmid	Relevant characteristic(s)	Source/reference
R. sphaeroides		
2.4.1	Wild type	W. Sistrom
RDXA1	Δ*rdxA*::ΩSp^r St^r	25
RDXB1	*rdxB*::ΩTp^r	This study
CCOP1	*ccoP*::ΩTp^r	This study
RDXBCCOP	Δ[*ccoP rdxB*]::ΩTet^r	This study
RDXABCCOP	Δ[*ccoP rdxB*]::ΩTet^r, Δ*rdxA*::ΩSp^r St^r	This study
CRTA1	*crtA*::ΩKm^r	This study
RDXB1CRTA1	*rdxB*::ΩTp^r, *crtA*::ΩKm^r	This study
CCOP1CRTA1	*ccoP*::ΩTp^r, *crtA*::ΩKm^r	This study
E. coli		
DH5α*phe*	(ϕ80d*lacZ*ΔM15) Δ*lacU169 recA1 endA1 hsdR17 supE44 thi1 gyrA96 relA1 phe*::Tn*10d*Cm	6
S17-1	Pro$^-$ Res$^-$ Mod$^+$ *recA*; integrated plasmid RP4-Tc::Mu-Km::Tn7	35
Plasmids		
pRK415	Mob$^+$ *lacZ*α Tc^r IncP	15
pBS	Ap^r	Stratagene
pHP45ΩTc	Source of ΩTc^r cassette	29
pHP45ΩKm	Source of ΩKm^r cassette	29
pUI1680	Derivative of pBS; Source of ΩTp^r cassette	J. Eraso
pSUP202/203	pBR325 Mob$^+$ Ap^r Cm^r Tc^r ColE1	35
pSUP202Km	pSUP202 (ΩKm in *Hin*dIII site of Tc^r gene)	S. Dryden
pSUP200Km	Sp^r St^r Km^r IncQ *puc*(URS + DRS)::*lacZYA′*	18
pCF250Km	Sp^r St^r Km^r IncQ *puc*(DRS)::*lacZYA′*	18
pUI1830	Sp^r St^r Tc^r IncQ *puf*::*lacZYA′*	L. Gong
pLX200	Sp^r St^r IncQ *bchF*::*lacZYA′*	10
pUI1957	~10-kb *Bam*HI fragment bearing *ccoNOQP* and *rdxBHI′* in pRK415	43
pUI1940	2,699-bp *Pst*I-*Pvu*II fragment from pUI1957 containing *rdxB* and *rdxH* in pBS	J. Zeilstra-Ryalls
pUI2800	Δ[*ccoP rdxB*]::ΩTet in pSUP202Km	This study
pUI2801	*ccoP*::ΩTp in pSUP203	This study
pUI2802	*rdxB*::ΩTp in pSUP203	This study
pUI2803	~5.3-kb *Bam*HI-*Eco*RI fragment from pUI1957 containing *ccoNOQP* in pRK415	This study
pUI2804	~7-kb *Cla*I-*Bam*HI fragment from pUI1957 containing *ccoQP* and *rdxBHI′* in pRK415	This study
pUI2805	~5.6-kb *Pst*I-*Bam*HI fragment from pUI1957 containing *rdxBHI′* in pRK415	This study
pUI2806	2,699-bp *Pst*I-*Pvu*II fragment from pUI1957 containing *rdxB* and *rdxH* in pRK415	This study
pUI2807	2,152-bp *Nar*I fragment from pUI1957 containing *rdxB* in pRK415	This study
pMS111	~3.5-kb *Bam*HI fragment containing *crtA* in pRK415	M. Sabaty
pUI2850	*crtA*::ΩKm in pSUP203	This study
pUI2851	1,356-bp *Sty*I fragment containing the *crtA* gene in pRK415	This study
pUI2711	Sp^r St^r IncQ *crtA*::*lacZYA′*	40

chromosome. RdxA is a membrane protein predicted, although not yet demonstrated, to coordinate two [4Fe-4S] clusters and thus may be involved in redox processes (25). In *Rhizobium meliloti*, the counterpart of *rdxA*, namely *fixG*, is essential for symbiotic nitrogen fixation (14). Significantly, disruption of *rdxA* did not affect the ability of *R. sphaeroides* 2.4.1 to grow diazotrophically. However, unlike the monocistronic *rdxA* gene, *rdxB* is the first gene of an apparent four-gene cluster analogous to the *fixGHIS* operon of *R. meliloti* (14). Recently, it has been proposed that in *Bradyrhizobium japonicum*, the homolog of the *rdxBHIS* operon in that organism, *fixGHIS*, is required for the assembly and/or stability of the cbb_3-type cytochrome oxidase encoded by the *fixNOQP* operon (28). The CcoN protein is believed to contain the active site of the cytochrome oxidase, while CcoO and CcoP are mono- and diheme cytochromes, respectively, involved in electron transfer to the active site. The function of CcoQ remains unclear.

Here, we have constructed known *rdxB* and *ccoP* chromosomal mutations, disabling both genes in combination or individually in order to further investigate their role(s) in photosynthesis gene expression. We describe evidence for the involvement of the gene products of both of these operons in regulation governing the relative accumulations of the Crts SE and SO under photosynthetic and diazotrophic growth conditions. We further reveal that under aerobic growth conditions, each of these pathways is normally involved in the transcriptional regulation of the *puc* and *puf* operons. The possible role(s) of each of these pathways in the regulation of photosynthesis gene expression and Crt biosynthesis is discussed.

MATERIALS AND METHODS

Bacterial strains, plasmids, and growth conditions. The strains and plasmids used in this work are described in Table 1.

Escherichia coli strains were grown at 37°C on LB medium (22) supplemented, when required, with the following antibiotics: tetracycline, 15 μg/ml; ampicillin, 50 μg/ml; kanamycin, 50 μg/ml; trimethoprim, 50 μg/ml; and streptomycin and spectinomycin, 50 μg/ml each.

R. sphaeroides 2.4.1 strains were grown at 30°C on Sistrom's medium A (3) containing succinate as the carbon source and supplemented as required with the following antibiotics: tetracycline, 1 μg/ml; kanamycin, 25 μg/ml; trimethoprim, 50 μg/ml; and streptomycin and spectinomycin, 50 μg/ml each. Chemoheterotrophic cultures were grown aerobically on a rotary shaker or sparged with 30% O_2-69% N_2–1% CO_2. Photosynthetic cultures were grown at a medium incident light intensity of 10 W/m^2 and sparged with 98% N_2–2% CO_2. Cultures grown diazotrophically were sparged with 98% N_2–2% CO_2 in the light (10 W/m^2) on a previously described modified Sistrom's medium containing no source of reduced nitrogen (25). N_2 and CO_2 gases were purchased from Iweco, Inc. (Houston, Tex.) and were 99.998 and 99.995% pure, respectively.

DNA manipulations, sequence determination, and analysis. Standard protocols or manufacturers' instructions were followed to isolate plasmid DNA, as well as for restriction endonuclease, DNA ligase, and other enzymatic treatments of

plasmids and DNA fragments. Enzymes were purchased from New England Biolabs, Inc. (Beverly, Mass.), Promega Corp. (Madison, Wis.), U.S. Biochemical Corp. (Cleveland, Oh.), and Boehringer Mannheim Biochemicals, Bethesda Research Laboratories (BRL) Life Technologies Inc. (Gaithersburg, Md.).

DNA sequencing from both strands was performed with an ABI 373A automatic DNA sequencer (Applied Biosystems, Inc., Foster City, Calif.) at the DNA Core Facility of the Department of Microbiology and Molecular Genetics, The University of Texas Health Science Center, Houston, Tex. Oligonucleotides used for priming standard sequencing reactions were synthesized at the DNA Core Facility of the Department of Microbiology and Molecular Genetics, The University of Texas Health Science Center, or were purchased from BRL Life Technologies. The primers used were the M13 universal and reverse sequencing primers, in addition to custom oligonucleotide primers which were designed to complete DNA sequence determination.

Conjugation techniques. Plasmids were mobilized in biparental matings from *E. coli* S17-1 strains into *R. sphaeroides* strains as described elsewhere (5).

Construction of *R. sphaeroides* 2.4.1 mutants. Disruption of the *ccoP* gene involved insertion of the ΩTp cassette into the *Pst*I site, which is 584 bp from the start of the structural gene (pUI2801). To disrupt *rdxB*, an ΩTp cassette was introduced into the *Eco*RI site 240 bp from the presumed start codon of the structural gene (pUI2802). The 763-bp fragment between the *Pst*I and *Eco*RI sites was replaced with an ΩTc cassette to disrupt *ccoP* and *rdxB* simultaneously (pUI2800). These constructs were cloned into pSUP203 or pSUP202Km and mobilized by conjugation into *R. sphaeroides* 2.4.1 or RDXA1 (25). In order to disrupt the *crtA* gene, an ΩKm cassette was inserted into a unique *Bst*EII site 518 bp from the start codon of the *crtA* gene (pUI2850), cloned into pSUP203, and crossed into the wild-type 2.4.1, RDXB1, and CCOP1 strains. The genomic structures of all mutant strains were confirmed by restriction mapping and Southern hybridization.

Southern hybridization analysis. Hybridizations were performed according to the protocol described for Quikhyb rapid hybridization solution (Stratagene). DNA probes were oligolabeled with [α-^{32}P]dCTP by using random primer (New England Biolabs) and Sequenase enzyme (U.S. Biochemical) as described elsewhere (31).

Crt and Bchl analyses. Photopigments were extracted with acetone-methanol (7:2 [vol/vol]) from cell pellets and quantitated as described previously (3). The acetone-methanol-extracted pigments were then concentrated for high-performance liquid chromatography (HPLC) analysis on a Shimadzu system equipped with an SPD-M10AV diode array detector as described by Yeliseev et al. (39).

Spectral analysis of membrane fractions. Crude cell-free lysates were prepared by sonication for 1 min in ICM buffer (10 mM KH_2PO_4, 1 mM EDTA; pH 7.2) with a Sonifier Cell Disrupter (Branson Sonic Power Co., Danbury, Conn.) followed by two rounds of centrifugation on a benchtop microcentrifuge at 13,000 rpm to remove cell debris. Spectra were recorded with a UV 1601PC spectrophotometer (Shimadzu Corp.). The B800-850 and B875 complex levels were determined by the method of Meinhardt et al. (24) from the spectral data collected.

β-Galactosidase assays. *R. sphaeroides* 2.4.1 cultures used for the determination of β-galactosidase activity were grown chemoheterotrophically with sparging of 30% O_2–69% N_2–1% CO_2 or photoheterotrophically with sparging of 98% N_2–2% CO_2 to an optical density at 660 nm of 0.15. The assays were performed on preparations of crude cell extracts as described elsewhere (37). Reagent-grade *o*-nitrophenyl-β-D-galactopyranoside, purchased from Sigma Chemical Co., was used as the substrate. The data provided are the averages of at least two independent determinations. β-Galactosidase units are defined as micromoles of *o*-nitrophenyl-β-D-galactopyranoside hydrolysed per minute per milligram of protein extract.

Determination of protein concentrations. Concentrations of protein in crude cell extracts used for spectral analysis or β-galactosidase activity assays were measured by the bicinchoninic acid protein assay (Pierce, Rockford, Ill.).

Nucleotide sequence accession number. The nucleotide sequences of the *rdxB* and *rdxH* genes, along with the 3′ sequence from *ccoP* and the 5′ sequence from *rdxI*, have been submitted to GenBank under accession number U67862.

RESULTS

DNA sequence determination of the *rdxB* and *rdxH* genes and their alignment. The *rdxB* gene was identified as a homolog of the *rdxA* gene and was partially sequenced in an earlier study (42). With plasmids encompassing the *ccoNOQP* and *rdxBHI* genes, pUI1957, and a subclone containing only the *rdxBH* genes, pUI1940, the complete DNA sequence of the *rdxBH* genes and flanking regions was determined for both strands by using specific oligonucleotide primers (Fig. 1). The *rdxB* gene is predicted to encode a protein of 477 amino acids and contains a potential FNR-binding consensus site 58 bp upstream of the presumed start codon. An alignment of the predicted amino acid sequences of RdxA and RdxB reveals 65% identity and 80% similarity. Residues in the RdxA protein which are predicted to form membrane-spanning domains (25) are highly conserved in RdxB. All 12 cysteine residues, including the 8 proposed to bind two [4Fe-4S] clusters, are fully conserved in both proteins. The predicted amino acid sequences for RdxB and RdxH were aligned with homologs from other bacteria by using the PILEUP program from the Genetics Computer Group software package of the University of Wisconsin. Overall, a high degree of conservation of these proteins across many bacterial species (Fig. 2A and B) is evident. The cysteine residues predicted to bind the iron-sulfur clusters are fully conserved in all proteins. In our earlier analysis of the RdxA protein using *phoA* fusions (25), we determined that the protein was likely to be membrane localized. Similarly, comparison of RdxA with other sequences in the database (25) further indicated that the protein was likely to contain two [4Fe-4S] centers and two potential half-centers. Because of the high degree of conservation between RdxB and RdxA, we have assumed similar structural features for the purpose of these studies, although this remains to be determined.

Construction of *rdxB* and *ccoP* mutations. The genomic organization of the *ccoNOQP* and *rdxBHIS* operons, together with the plasmids used in the construction of the *rdxB* and *ccoP* mutations, is depicted in Fig. 3A and B. The methodology employed for plasmid construction and mutant selection is outlined in Materials and Methods. When grown on SIS agar plates in the presence of O_2, all mutations in *rdxB* or *ccoP* gave rise to colonies with very deep red pigmentation, compared with the pale red coloration of wild-type 2.4.1 and RDXA1. This phenotype is similar to that observed for the *R. sphaeroides* 2.4.1 strain bearing a transposon mutation between the *ccoN* and *ccoO* genes (43) and was the first indication that known mutations in both *ccoNOQP* and *rdxBHIS* may result in similar phenotypes.

NADI analysis of cytochrome oxidase activity in RDXB1 and CCOP1. The mutant strains were tested for cytochrome oxidase activity by using the NADI reaction (α-naphthol plus dimethyl-*p*-phenylenediamine plus $O_2 \rightarrow$indophenol blue plus H_2O) (23). Colonies with cytochrome oxidase activity rapidly stain a deep blue due to the production of indophenol blue. As expected, wild-type 2.4.1 colonies were observed to turn blue in the first 1 to 2 min after the plates were flooded with NADI reagent. In contrast, the CCOP1 mutant strains were observed to test NADI negative during the first 15 min of the reaction. The slow development of blue coloration after this time can be attributed to cytochrome aa_3 oxidase, which is intact in all of the strains tested. Interestingly, like the wild type, the RDXA1 and RDXB1 mutant strains were all found to be NADI positive, thus indicating that the cbb_3-type cytochrome oxidase activity is unaffected in these mutants under the conditions tested. Under the growth conditions examined in this study, all mutant strains grew at rates comparable to those observed for 2.4.1.

RDXB1 and CCOP1 mutants accumulate high levels of SO during anoxygenic photosynthetic and diazotrophic growth. The sequence similarity between RdxB and the FixG protein from *R. meliloti*, which is essential for symbiotic nitrogen fixation (14), together with the observation that the *rdxA* null mutation constructed previously remains unaffected in its capacity to fix atmospheric nitrogen (25), prompted us to examine the abilities of RDXB1 and CCOP1 mutants to grow diazotrophically. All mutant strains examined, including the triple mutation lacking *rdxA*, *rdxB*, and *ccoP*, remained capable of diazotrophic growth at rates comparable to those for 2.4.1 and RDXA1.

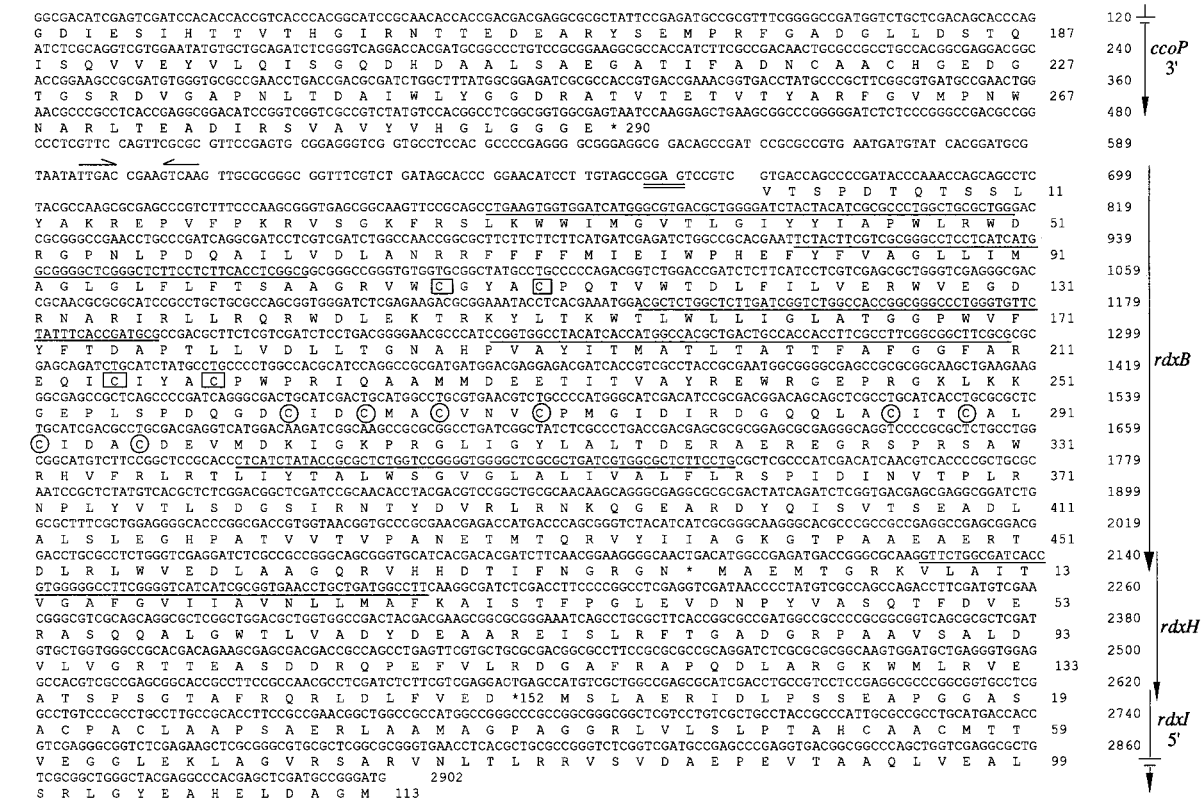

FIG. 1. Nucleotide and predicted amino acid sequences of the *rdxB* and *rdxH* genes. Upstream of *rdxB*, a potential Shine-Dalgarno sequence is doubly underlined, and a putative FNR-binding domain is indicated by arrows above the DNA sequence. Predicted transmembrane domains within *rdxB* and *rdxH* are underlined, and the eight cysteine residues in the predicted amino acid sequence of RdxB proposed to bind two 4Fe-4S clusters are circled. The remaining four cysteine residues which may also bind iron sulfur centers are boxed. Upstream of *rdxB*, sequence from the 3′ end of the *ccoP* gene is provided, and downstream of *rdxH*, sequence from the 5′ end of *rdxI* is shown.

However, during the course of these experiments, we did observe that the pigment content of the mutant strain(s) was visibly altered during anoxygenic diazotrophic and, to a lesser degree, photosynthetic growth. Under these growth conditions, wild-type cultures are green-brown due to the presence of high levels of Bchl and the reduced Crt, SE. RDXA1 has the same appearance as 2.4.1. In contrast, the RDXB1, CCOP1, RDXBCCOP, and RDXABCCOP strains were deep red under these same growth conditions. A visible red is associated with high levels of the oxidized Crt, SO, which in the wild type primarily accumulates under aerobic and semiaerobic growth conditions.

To examine the Crt compositions of 2.4.1 and the mutant strains, photopigments were extracted and spectral analysis was performed. The levels of Bchl and Crt from strains grown photosynthetically and diazotrophically are shown in Table 2. Measurement of the relative amounts of SE and SO in the photopigments was determined by HPLC analysis. Under photosynthetic growth conditions, SE is the major Crt in 2.4.1 and RDXA1 cultures, while in all of the RDXB1 and CCOP1 cultures, approximately equal concentrations of SE and SO accumulate. Under these growth conditions, the SE-SO ratio in the RDXABCCOP mutant represents an approximately 15-fold change from that in wild-type 2.4.1. Although this pattern is repeated in diazotrophically grown cultures, the effect is much more dramatic particularly in the RDXBCCOP and RDXABCCOP cultures, in which SE levels decrease to 13 and 8%, respectively, of the total Crt. For the RDXABCCOP mutant, this represents more than a 50-fold change in the SE-SO ratio from wild-type 2.4.1, in which SE is approximately 82% of the total Crt. It has previously been proposed that either CrtA activity or formation responds to a redox signal (39). The data presented here suggest that under anoxygenic conditions, mutations in the *rdxB* and *ccoP* genes also affect CrtA structure and/or function. Finally, the actual levels of SE and SO accumulated (Table 2) appear to be approximately the same in the mutant strains, regardless of the number of mutations present.

In order to test whether increased CrtA activity in the RDXB1 and CCOP1 mutants was the result of alterations manifest at either the transcriptional or posttranscriptional levels, the levels of *crtA* transcription under anaerobic photosynthetic conditions for the wild-type and mutant strains were determined with the *crtA*::*lacZ* fusion plasmid pUI2711 (40). This analysis demonstrated that expression of *crtA* in the RDXB1 (2,060 ± 160 β-galactosidase units) and CCOP1 (2,152 ± 224 β-galactosidase units) mutants was approximately 60% higher than that observed for wild-type 2.4.1 (1,314 ± 66.9 β-galactosidase units). In other studies, we have shown that *crtA*::*lacZ* levels can change by as much as fivefold (40), and thus the changes observed here do not suggest a major transcriptional effect on *crtA* gene expression in these mutant strains. Therefore, because of the very large oscillations in SO accumulation in the mutant strains, we believe that the effect of the *rdxB* and *ccoP* mutations on SO accumulation is primarily at the posttranscriptional level.

Complementation of RDXB1 and CCOP1 mutants. Plasmids bearing DNA fragments containing genes from the *cco NOQP* and *rdxBHIS* operons were introduced in trans to com-

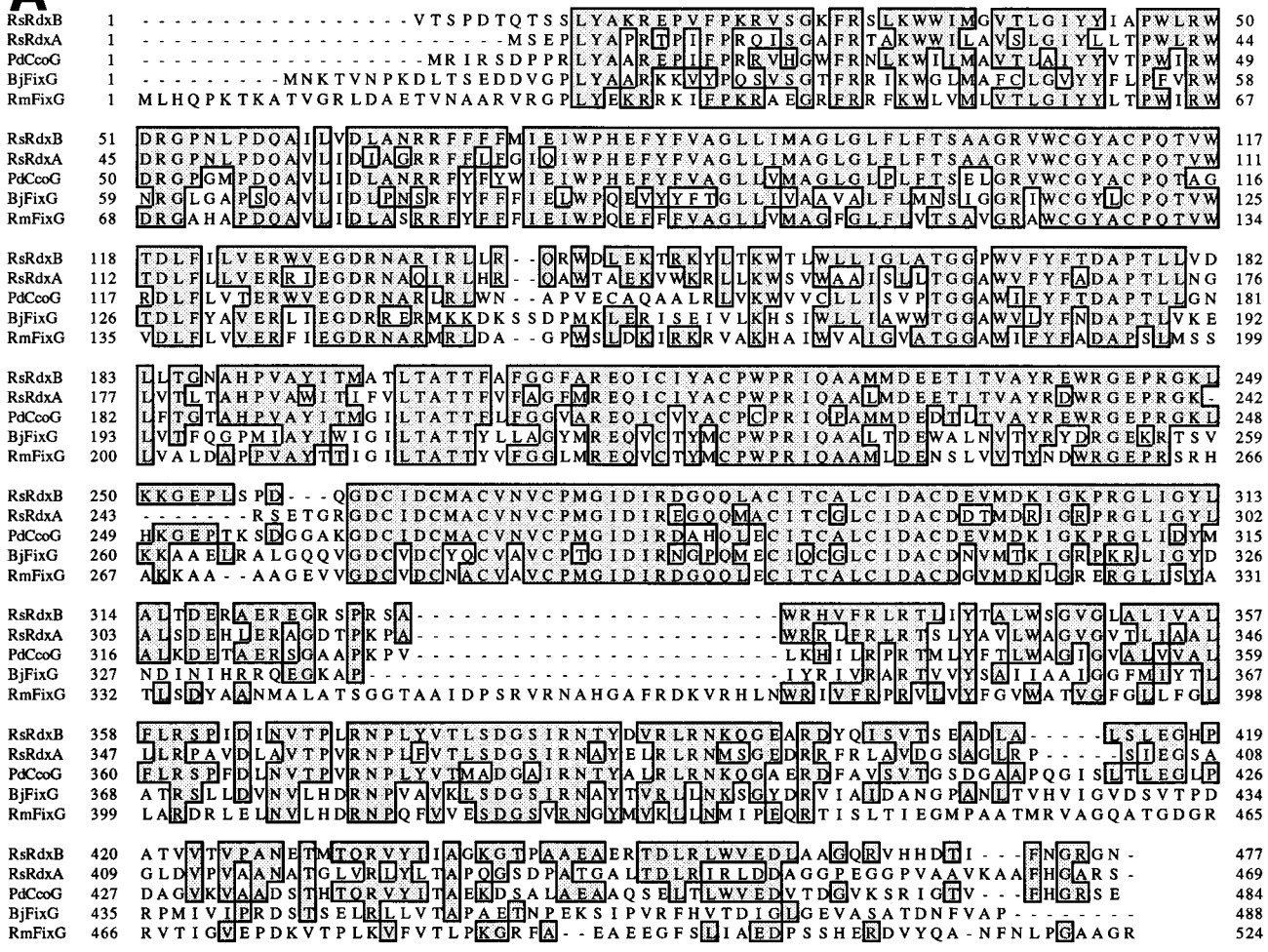

FIG. 2. Predicted protein sequences and alignments of the *rdxB* and *rdxH* gene products. (A) The predicted amino acid sequence of the *rdxB* gene aligned with other *rdxB* homologs. RsRdxB, *R. sphaeroides* 2.4.1 RdxB; RsRdxA, *R. sphaeroides* 2.4.1 RdxA; PdCcoG, *Paracoccus denitrificans* CcoG; BjFixG; *B. japonicum* FixG; RmFixG, *R. meliloti* FixG. All residues showing homology with RdxB residues are shaded. (B) The predicted amino acid sequence of the *rdxH* gene aligned with those of other *rdxH* homologs. RsRdxH, *R. sphaeroides* 2.4.1 RdxH; BjFixH, *B. japonicum* FixH; RmFixH, *R. meliloti* FixH.

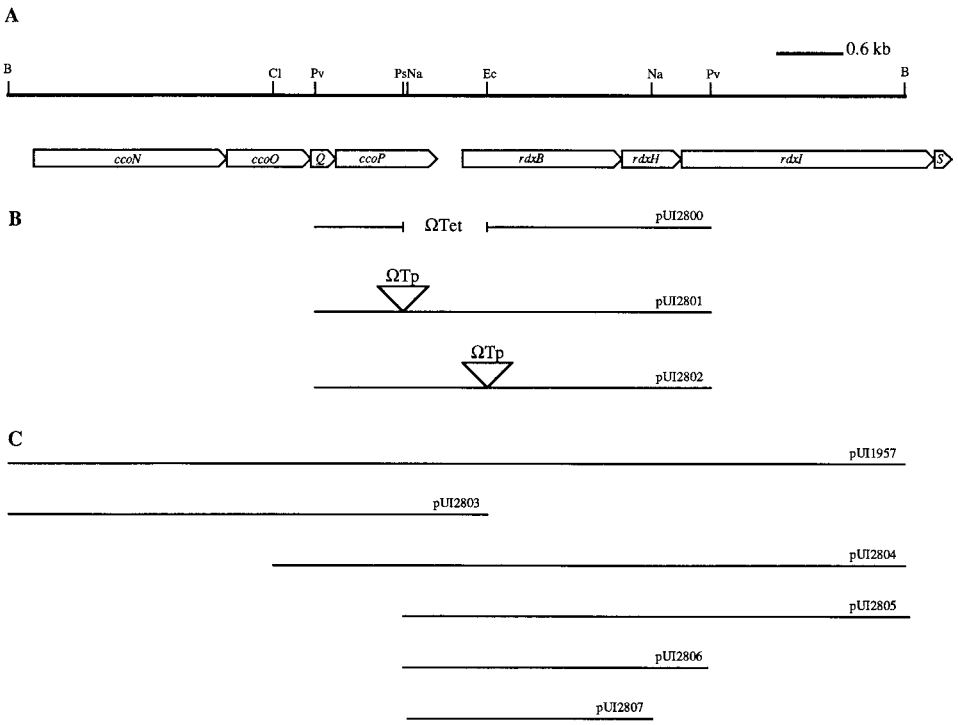

FIG. 3. Physical map of the *R. sphaeroides ccoNOQP rdxBHIS* region. (A) Restriction map (at top) of the DNA encompassing the *cco* and *rdx* chromosomal region. Restriction sites: B, *Bam*HI; Cl, *Cla*I; Pv, *Pvu*II; Ps, *Pst*I; Na, *Nar*I; Ec, *Eco*RI. (B) Plasmids used to construct *rdxB* and *ccoP* chromosomal mutations. The Ω cassettes were inserted at the positions indicated. (C) Chromosomal fragments from the *cco* and *rdx* region used to complement the *rdxB* and *ccoP* mutations. All fragments were introduced in trans on vector pRK415.

plement the RDXB1 and CCOP1 mutants (Fig. 3C; Table 3). All strains were grown diazotrophically, and successful complementation was defined as the restoration of SE and SO levels to approximately those found in 2.4.1. In addition, we observed that normal wild-type coloration was restored to the mutant strains growing on the surface of SIS agar plates, suggesting restored control of *puc* and/or *puf* operon expression in the presence of oxygen (see below). Complementation of the RDXB1 and RDXAB mutant strains required both the *rdxB* and *rdxH* genes in trans, suggesting that expression of *rdxH* was affected by the disruption of *rdxB*. However, the *rdxIS* genes were not required for successful complementation, indicating either the presence of a secondary promoter between *rdxH* and *rdxI* or that the absence of the *rdxIS* gene products was not involved in the phenotypes observed. Introduction of the *ccoQ* and *ccoP* genes was sufficient to complement the CCOP1 mutant, although it is important to note that these genes can be expressed from the tetracycline resistance gene promoter on the plasmid. Nonetheless, expression of *ccoNO* in the mutant strains appears to be normal. Complementation of RDXBC COP and RDXABCCOP was achieved by introduction of the *ccoNOQP* and *rdxBHI* genes in trans. Finally, no complementation of the CCOP1 mutant by the *rdxBHI* genes was observed, nor was the RDXB1 mutant complemented by *ccoNOQP*. Thus, mutations in either *rdxB* or *ccoP* independently affect SO accumulation.

Disruption of the *crtA* gene in 2.4.1, RDXB1, and CCOP1. The DNA sequence and genomic organization of the *R. sphaeroides crtA* gene have previously been determined (17), and the *crtA* gene was recently cloned from *R. sphaeroides* 2.4.1 on a

TABLE 2. Levels of photopigments in *R. sphaeroides* 2.4.1 strains[a]

Strain	Value for photosynthetic cultures					Value for diazotrophic cultures				
	Bchl	Crt	SE	SO	SE/SO[b]	Bchl	Crt	SE	SO	SE/SO[b]
2.4.1	57.8 ± 1.15	12.9 ± 0.40	11.7 ± 0.70	1.2 ± 0.02	9.75	29.7 ± 3.05	7.7 ± 0.79	6.30 ± 0.85	1.4 ± 0.07	4.50
RDXA1	47.3 ± 1.70	12.7 ± 0.26	11.4 ± 0.28	1.2 ± 0.04	9.50	23.3 ± 3.02	7.3 ± 0.63	5.90 ± 0.60	1.4 ± 0.06	4.21
RDXB1	48.5 ± 3.00	12.2 ± 1.13	6.90 ± 1.06	5.3 ± 0.30	1.30	31.1 ± 4.97	7.2 ± 0.51	2.70 ± 0.28	4.5 ± 0.64	0.60
RDXAB	44.1 ± 4.01	12.1 ± 1.36	6.30 ± 0.91	5.8 ± 0.45	1.08	20.5 ± 2.05	6.5 ± 0.32	1.30 ± 0.36	5.2 ± 0.36	0.25
CCOP1	42.1 ± 4.97	10.6 ± 1.67	4.40 ± 0.61	6.2 ± 1.08	0.70	35.4 ± 2.61	8.4 ± 0.50	2.02 ± 0.16	6.4 ± 0.45	0.31
RDXBCCOP	50.2 ± 3.01	9.30 ± 1.40	4.90 ± 1.80	4.4 ± 0.50	1.11	32.4 ± 3.95	6.3 ± 0.21	0.80 ± 0.30	5.5 ± 0.17	0.15
RDXABCCOP	35.4 ± 6.01	7.30 ± 0.87	3.22 ± 0.15	4.1 ± 1.00	0.78	19.6 ± 0.90	4.7 ± 0.16	0.40 ± 0.24	4.3 ± 0.17	0.09

[a] Strains were grown photoheterotrophically in the light (10 W/m^2) with sparging of 98% N_2–2% CO_2 to an A_{660} of 1.0. Photosynthetic cultures were grown in Sistrom's minimal medium, and diazotrophic cultures were grown in the same medium lacking reduced nitrogen sources. All values provided are the averages of at least two independent determinations, and deviations from the means are indicated. Photopigment values are micrograms per 10^{10} cells.

[b] Ratio of SE to SO as determined by HPLC analysis of Crt composition.

TABLE 3. Crt composition (SE-to-SO ratio) in complemented RDXB1 and CCOP1 mutants[a]

Plasmid	Relevent gene(s)	Value for the following strains:					
		2.4.1	RDXB1	RDXAB	CCOP1	RDXBCCOP	RDXABCCOP
pRK415	Control	6.9	0.71	0.65	0.05	0.17	0.32
pUI1957	*ccoNOQP* and *rdxBHI*	4.2	4.65	3.31	5.41	6.95	3.23
pUI2803	*ccoNOQP*	ND[b]	0.67	0.28	3.34	ND	ND
pUI2804	*ccoP* and *rdxBHI*	ND	ND	ND	5.23	ND	ND
pUI2805	*rdxBHI*	ND	5.65	4.22	0.08	ND	ND
pUI2806	*rdxBH*	ND	4.37	3.43	ND	ND	ND
pUI2807	*rdxB*	ND	0.46	0.38	ND	ND	ND

[a] Strains were grown diazotrophically in Sistrom's minimal medium supplemented with tetracycline (1 μg/ml) to an A_{660} of 0.5.
[b] ND, not determined.

3.5-kb *Bam*HI fragment (pMS111) (30). In order to determine if the increased SO accumulation in the mutant strains was dependent on a functional CrtA, the *crtA* gene was disrupted in the wild-type 2.4.1, RDXB1, and CCOP1 strains (Fig. 4) as described in Materials and Methods. As expected, disruption of *crtA* in the wild-type and mutant backgrounds prevented the accumulation of SO. Thus, CrtA minus strains are green when grown semiaerobically on SIS agar plates. Similarly, HPLC analysis of CRTA1, RDXB1CRTA1, and CCOP1CRTA1 mutant strains grown under photosynthetic growth conditions revealed the complete absence of SO. A 1,356-bp *Sty*I fragment containing the *crtA* gene carried on plasmid pRK415 (pUI2851) was used to complement the CRTA1 mutant strains. Complementation restored wild-type, red pigmentation in colonies grown semiaerobically on SIS agar plates, and the production of SO under photosynthetic growth conditions was demonstrated by HPLC analysis. Thus, the effect of mutations in *rdxB* and *ccoP* on SO accumulation appears to operate exclusively through *crtA* or, more likely, its gene product.

Oxygen repression of photosynthetic membrane formation in RDXB1 and CCOP1. The observation by Zeilstra-Ryalls and Kaplan (43) that a transposon insertion between the *ccoN* and *ccoO* genes led to the synthesis of the photosynthetic apparatus in the presence of high oxygen, coupled with our observation that CCOP1 and RDXB1 mutants were deeply pigmented compared to 2.4.1 when grown semiaerobically on SIS agar, led us to more closely examine aerobically grown cultures of the RDXB1 and CCOP1 mutants. Membrane fractions from cultures grown in the presence of 30% oxygen were prepared, and spectral analysis was performed (Fig. 5). All of the RDXB1 and CCOP1 mutants, either singly or in combination, were found to synthesize photosynthetic complexes, compared with wild-type 2.4.1 and RDXA1. This is consistent with our observation that these mutants have deep red pigmentation compared to that of 2.4.1 and RDXA1. The levels of B800-850 and B875 spectral complexes were not significantly different in the RDXB1 and CCOP1 mutants grown under 30% oxygen. On average, levels of B800-850 were 0.22 (± 0.07) nmol/mg of protein, while B875 levels were 1.14 (± 0.28) nmol/mg of protein. This compared with levels of B875 and B800-850 which were essentially background in wild-type 2.4.1 and RDXA1. Predictably, HPLC analysis of pigments extracted from mutant cells grown aerobically demonstrated that the Crt content of the photosynthetic complexes was exclusively SO. The levels of B800-850 and B875 varied little in any of the RDXB1 and CCOP1 mutants, and this is consistent with the observation that mutations in *rdxB* or *ccoP* also gave rise to a similar phenotype under photosynthetic and diazotrophic growth conditions. Whereas we only suspected that the original transposon insertion isolated by Zeilstra-Ryalls and Kaplan (43) resulted in a null phenotype for the cbb_3 complex, the CCOP1 mutants employed here leave little doubt that the relevant membrane complex is defective.

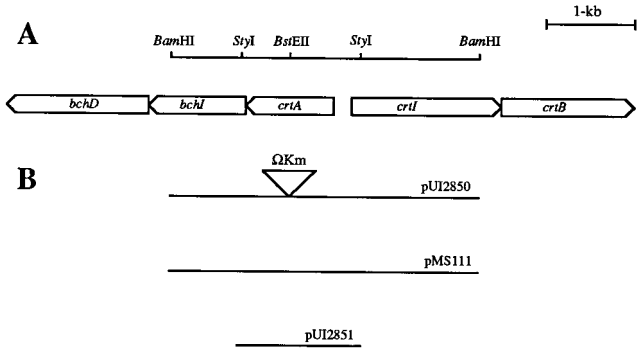

FIG. 4. Physical map of the *R. sphaeroides crtA* region. (A) Restriction map (top line) of the DNA in the region of the *crtA* gene. (B) Plasmids used in the construction and complementation of the *crtA* chromosomal mutation. The ΩKm cassette was inserted into the *Bst*EII site of the *crtA* gene.

Analysis of *puc*, *puf*, and *bchF* expression in RDXB1 and CCOP1. The presence of photosynthetic light-harvesting complexes in the presence of oxygen raised the question of whether the level of transcription of the genes encoding the B800-850 and B875 structural polypeptides (encoded by *puc* and *puf* operons, respectively) had been elevated. To address this question, we assessed the transcriptional activities of the *puc* and *puf* operons using transcriptional fusions to *lacZ*. The data, presented in Fig. 6 and Table 4, show a greater-than-10-fold increase in the levels of *puc* transcription (pCF200Km) in all of the mutants compared with wild-type 2.4.1. This represents a substantial increase in *puc* operon expression and approaches the level of *puc* transcription observed under anoxygenic photosynthetic conditions (18), i.e., *puc* operon expression is derepressed. The level of *puc* operon expression in RDXA1 was not significantly different from that for the wild type, and this was consistent with the absence of aerobic spectral complex formation in this strain.

The fact that mutations in the *rdxB* and *ccoP* genes affected the level of *puc* transcription with plasmid pCF200Km raised several interesting questions about what transcription factors may be involved and their site of action. To assess the site of action of the *puc* regulatory sequence involved in this response, we tested the *puc*::*lacZ* reporter pCF250Km. This reporter contains only 92 bp of DNA sequence upstream of the start site of transcription of the *puc* operon, whereas pCF200Km contains 629 bp of DNA sequence upstream of the transcription start site (Fig. 6). Thus, pCF250Km differs from pCF200Km in

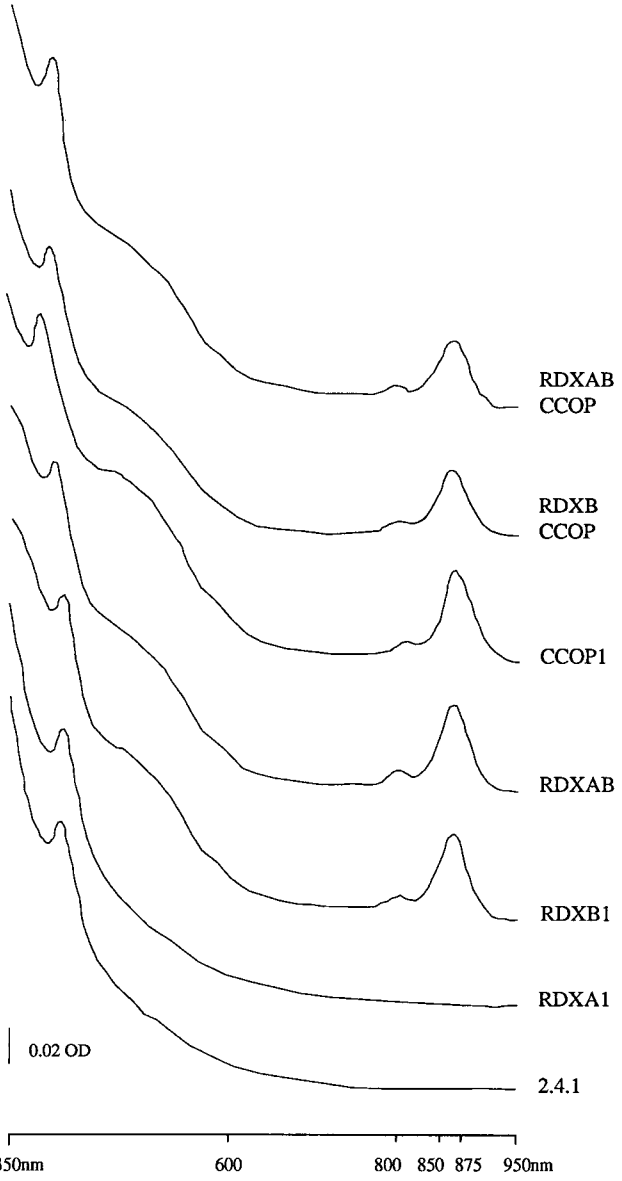

FIG. 5. Absorbtion spectra of membranes of *R. sphaeroides* 2.4.1, RDXA1, RDXB1, CCOP1, RDXAB, RDXBCCOP, and RDXABCCOP strains. Cultures were grown chemoheterotrophically with sparging of 30% O_2–69% N_2–1% CO_2 to an A_{660} of 0.15. All samples contain 1 mg of protein per ml.

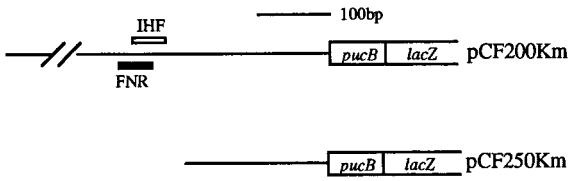

FIG. 6. Transcriptional fusion plasmids. The relative endpoints of the 5′ upstream DNA sequence of the *puc* operon contained in the *lacZ* fusion plasmids pCF200Km and pCF250Km are depicted. The locations of the IHF binding site and the potential FNR consensus sequence are highlighted. See Table 4 for β-galactosidase activities for *R. sphaeroides* strains bearing these plasmids.

having only the downstream regulatory sequences (DRS) involved in control of *puc* activity and lacks the upstream regulatory sequences (URS) required for enhanced expression of the *puc* operon (18–20). The binding site for integration host factor (IHF) and the potential FNR consensus sequence occur in the region upstream of the DRS.

When *puc* activity in RDXB1 and CCOP1 was measured with pCF250Km, an approximately fourfold increase in *lacZ* expression above wild-type 2.4.1 levels was detected (Table 5). Thus, mutations in either *rdxB* or *ccoP* resulted in the derepression of *puc* operon expression, but the full extent of the increased transcriptional activity required sequences upstream and downstream of the IHF and FNR-binding consensus sequences.

Analysis of *puf*::*lacZ* expression in RDXB1 and CCOP1 mutants with the reporter plasmid pUI830 also revealed a fourfold increase in activity (Table 5). These values for the levels of *puf* transcriptional activity are similar to those found under anaerobic conditions (43). Levels of *puf* operon expression in RDXA1 were essentially the same as those observed for the wild type. Thus, both *puc* and *puf* transcriptional activities are affected in the CCOP1, RDXB1, and double mutant strains to approximately the same extent. It appears that both *cco* and *rdxB* reside in the same regulatory pathway. On the other hand, the *rdxA* mutation does not appear to have any effect on these genes at the transcriptional level.

However, the relatively low levels of B800-850 and B875 spectral complexes in the mutant strains found under aerobic conditions were inconsistent with the high levels of transcription of the *puc* and *puf* operons, suggesting that other limitations precluded the presence of high levels of spectral complexes. We know from our studies with mutant PRRB78 having a Leu→Pro change at position 78 in the sensor kinase known to be involved in photosynthesis gene expression that high levels of spectral complexes can be formed aerobically (7). To address this question, we measured the transcriptional activity of the *bchF* gene promoter fused to *lacZ* (pLX200) in the RDXB1 and CCOP1 mutant strains. The data, shown in Table 5, demonstrated that expression of *bchF* was relatively unchanged in the mutant strains compared with that for 2.4.1, suggesting that transcription of *bchF*, at least, is not increased by the mutations in the *rdxB* and *ccoP* genes. Furthermore, although it is possible that Bchl may be limiting for spectral complex formation in the RDXB1 and CCOP1 mutants under aerobic growth conditions, it is also well documented that the final cellular levels of spectral complexes are controlled at the posttranscriptional level (11, 12, 21, 26, 36, 39), which can be independent at the level of Bchl.

DISCUSSION

Here, we present evidence for the involvement of the *cco NOQP* and *rdxBHIS* gene products in the regulation of photosynthesis gene expression in response to changing oxygen tensions. Further, we have demonstrated that disruption of the *rdxB* or *ccoP* gene leads to increased levels of SO relative to SE under anoxygenic photosynthetic and diazotrophic growth conditions. This effect is at the posttranscriptional level rather than at the level of transcription of the *crtA* gene.

The effect of mutation of the *cco* operon on photosynthesis gene expression and SO accumulation appears to involve changes in either cellular redox poise or the accumulation of a critical redox intermediate, as judged by the loss of a NADI-positive reaction. Structural alterations involving membrane topology cannot be eliminated as a causal event. On the other hand, the role of *rdxB*, *rdxH*, or both in these same control mechanisms is more difficult to ascribe to alterations in redox

TABLE 4. β-Galactosidase activities of cell extracts of *R. sphaeroides* 2.4.1 strains bearing *puc*::*lacZ* transcriptional fusion plasmids[a]

Plasmid	β-Galactosidase activity for the following strains:						
	2.4.1	RDXA1	RDXB1	CCOP1	RDXAB	RDXBCCOP	RDXABCCOP
pCF200Km	191 ± 13	283 ± 28	2,577 ± 214	2,332 ± 134	2,212 ± 102	1,923 ± 67	1,952 ± 147
pCF250Km	188 ± 29	ND	609 ± 41	596 ± 16	ND	ND	ND

[a] The strains were grown aerobically, sparging with a gas mixture of 69% N_2–30% O_2–1% CO_2 to an A_{660} of 0.15 in Sistrom's minimal medium supplemented with kanamycin (25 μg/ml). The values for β-galactosidase activity are the averages of at least three independent determinations and are micromoles per minute per milligram of protein. Standard deviations were <16%. ND, not determined. See Fig. 6 for plasmid diagrams.

activities, since no direct evidence exists to prove such a relationship. However, the body of evidence which has accumulated makes this a reasonable alternative. First, there is the comparative relationship between RdxB, RdxA, and other known proteins believed to harbor two [4Fe-4S] clusters (25) which often are involved in redox reactions. We have also demonstrated that the conversion of SE to SO is regulated at the posttranscriptional level by a variety of environmental parameters which would have in common a redox-mediated or -regulated conversion of SE to SO (39). More recent evidence indicates that this conversion, particularly under anaerobic conditions, is exceedingly complex (41). Whereas it has been demonstrated that molecular O_2 is the source of the 2-oxo group of SO formed aerobically (33), this cannot be true anaerobically. We know that molecular O_2 is not present, as judged by the purity of the gas mixtures used to sparge the cultures used here; moreover, the growth of cells under diazotrophic conditions further precludes the presence of O_2, and, finally, we were unable to detect free O_2. We have also shown that H_2O is not the source of the 2-oxo group introduced during the conversion of SE to SO under anaerobic conditions (41). Therefore, it appears that an organic source of O_2 is required for this reaction, and this may explain the inability to demonstrate this reaction in vitro under anaerobic conditions.

Thus, we are left with the fact that the conversion of SE to SO is apparently under strong redox influence and that Cco and RdxB can affect the balance of this reaction presumably at the posttranscriptional level, which in itself is a significant observation. Given that Cco mutants are NADI minus, the most likely role of RdxBH in these observations is because of its role in a redox-related pathway, although this has not been directly proven. Nonetheless, the remainder of this discussion will proceed based on this assumption.

Because the cbb_3 pathway interacts directly with O_2, we suggest that RdxBH and perhaps RdxIS are downstream elements in this redox-dependent pathway. This is similar but not identical to the situation in *B. japonicum*, in which disruption of the *fixP* gene and deletion of the *fixGHIS* operon (*R. sphaeroides rdxBHIS*) both serve to decrease cytochrome oxidase activity under microaerobic and anaerobic growth conditions (28, 44). Here, mutations in *rdxB* do not appear to affect the NADI reaction. Furthermore, complementation experiments demonstrated that mutations in *ccoP* cannot be complemented by *rdxB* and vice versa, thus providing additional evidence that the *rdx* and *cco* gene products, although independent of each other, reside in the same regulatory pathway. This is also borne out by the fact that mutations in either or both of these loci lead to essentially identical quantitative results, regardless of whether photosynthesis gene expression or SE and SO levels are measured. Thus, in *R. sphaeroides*, the results of NADI tests under semiaerobic growth conditions and SO accumulation under anaerobic photosynthetic and diazotrophic growth conditions suggest that although the RdxBHIS and CcoNOQP complexes are functionally independent, they are both members of the same regulatory pathway. It is also clear that neither CcoNOQP, RdxBHIS, nor RdxA appears to be obligatory for nitrogen fixation.

The homolog of *rdxI* in rhizobial species, *fixI*, is predicted to be an ATPase (14, 28), and in *B. japonicum* it has been proposed that FixI may encode a copper transport ATPase which, as part of the FixGHIS complex, may be involved in copper transport and its use for the cbb_3-type heme-copper oxidase (28). In *R. meliloti*, *fixS* has been designated as a gene although its function, if any, is unknown (14). The observation that the *rdxI* and *rdxS* genes were not apparently required for complementation of the *rdxB* mutation suggests either that an internal promoter within the operon may permit expression of these genes even after the insertion of the Ω cassette in *rdxB* or that neither gene product is required for the effective regulation of ICM repression or the conversion of SE to SO. It is impossible to choose between these alternatives at this time.

The disruption of *rdxA* does not appear to contribute appreciably to the phenotype in any of the mutants, and this raises further questions as to its function. The inability of *rdxA* to compensate for the absence of *rdxB* also points to a significant role for the *rdxHIS* genes. In contrast to *rdxB*, no FNR-binding consensus site exists upstream of *rdxA*, which suggests that regulation of its expression is quite different from that of *rdxBHIS*. We know that *rdxA* is expressed aerobically and anaerobically (25), and yet no detectable phenotype can be attributed to *rdxA* under either of these conditions.

Zeilstra-Ryalls and Kaplan (43) presented a model for the anaerobic regulation of photosynthesis gene expression which proposes that one or other of the Prr and FnrL systems or both may respond directly to the presumed changing redox signals generated by the membrane proteins encoded by the *cco NOQP* genes, which in turn respond to changing environmental conditions. Here, we demonstrated increased *puc* and *puf* operon transcriptional activity under aerobic conditions when

TABLE 5. β-Galactosidase activities from cell extracts of *R. sphaeroides* 2.4.1 strains bearing *puf*::*lacZ* (pUI1830) or *bchF*::*lacZ* (pLX200) transcriptional fusion plasmids[a]

Strain	β-Galactosidase activity[b]	
	pUI1830	pLX200
2.4.1	98 ± 10	427 ± 68
RDXA1	134 ± 2	ND[c]
RDXB1	423 ± 36	435 ± 15
CCOP1	371 ± 31	526 ± 38

[a] The strains were grown aerobically, sparging with a gas mixture of 69% N_2–30% O_2–1% CO_2 to an A_{660} = 0.15 in Sistroms minimal medium supplemented with antibiotics as appropriate.

[b] Micromoles of *o*-nitrophenyl-β-D-galactopyranoside hydrolyzed per minute per milligram of protein extract. The values are the averages of at least two independent determinations. Standard deviations were <16%.

[c] ND, not determined.

either RdxB or CcoP was disrupted. Additionally, it was observed that elevated *puc* expression in the mutants through the DRS was considerably enhanced by the presence of the URS in the *puc* reporter operon. The involvement of FnrL seems plausible when one considers that FnrL is likely to regulate expression of the *ccoNOQP* and *rdxBHIS* operons and that the *fnrL*, *ccoNOQP*, and *rdxBHIS* genes are clustered on the chromosome (42).

It is also significant that both the *puc* operon and the *bchF* gene are regulated by the transcriptional repressor PpsR (10). Two PpsR binding sites exist in the DRS of the *puc* promoter region, and we have demonstrated that increased expression of *puc* in the RDXB1 and CCOP1 mutants can act in part through the DRS. However, expression of *bchF* appears to be unaffected in the RDXB1 and CCOP1 mutant strains. It may be inferred, therefore, that PpsR is not the responsive agent in regulating gene expression in mutant strains altered in RdxB and CcoP. Thus, if derepressed photosynthesis gene expression in the RDXB1 and CCOP1 mutant strains does not act through PpsR, by elimination this suggests the FnrL and/or Prr system. Studies currently under way are designed to determine the relationships between Cco and RdxB in the presence and absence of the Prr and FnrL regulatory systems. By a similar analysis, we can eliminate the TspO regulatory system (40), since this system does not affect *puf* operon expression, which as shown here is derepressed in the RDXB1 and CCOP1 mutant strains in the presence of O_2.

Therefore, when taken together, all of the data indicate that cbb_3 and RdxBH may comprise a signal transduction pathway together with the Prr two-component system to affect photosynthesis gene expression in response to changes in O_2 availability. Further, FnrL may be involved in regulating *puc* operon expression either directly or indirectly. Direct involvement may be due to the presence of an FNR-binding consensus sequence within the URS of the *puc* operon, and indirect involvement of FnrL may be through its potential regulation of *ccoNOQP* and *rdxBHIS*, as well as other genetic elements in *hem* and *bch* gene expression.

In *R. sphaeroides* cultures growing under microaerobic conditions, the cbb_3 oxidase is the predominant cytochrome *c* oxidase (8), while under high O_2 tensions, the aa_3 oxidase becomes dominant (13). In rhizobial species, the *fixNOQP* operon (analogous to *ccoNOQP*) is also predicted to encode a high-affinity oxidase employed by the cell when growing symbiotically in root nodules (2, 4, 27). Expression of the *R. meliloti fixN* gene is induced under microaerobic conditions and not under high oxygen tensions (4). By contrast, in *R. capsulatus* which does not contain an aa_3-type oxidase, the oxidase encoded by the *ccoNOQP* operon is the major cytochrome oxidase under standard aerobic growth conditions (38). Interestingly, recent experiments in our laboratory have demonstrated that in an *R. sphaeroides* 2.4.1 mutant lacking the aa_3-type cytochrome oxidase subunit I encoded by the *ctaD* gene, the photosynthetic apparatus is not induced in cells grown aerobically (9). Thus, alterations in the cbb_3-type oxidase but not the aa_3-type oxidase appear to have a role in the generation of a cellular redox state or redox intermediate through which photosynthesis gene expression can be regulated.

Thus, major unanswered questions remain. What is the nature of the redox carrier or signal which is generated by a functional cbb_3 oxidase and, presumably, by the RdxBH system and which helps to mediate O_2 control of photosynthesis gene expression? How is this signal transmitted to the regulatory protein(s) involved in the regulation of photosynthesis gene expression? How does this regulatory protein(s) respond to this signal transduction pathway? How does the cellular redox poise serve to control CrtA function, which is reflected in the cellular abundance of SO relative to SE? Despite these significant gaps in our understanding of this complex regulatory system, it seems that the outlines of a regulatory model are beginning to appear.

ACKNOWLEDGMENTS

We thank J. Zeilstra-Ryalls for invaluable discussions throughout this study and A. Yeliseev for assistance with HPLC analysis.

This work was supported by USPHS research grant GM15590 to S.K.

REFERENCES

1. **Armstrong, G. A., M. Alberti, F. Leach, and J. E. Hearst.** 1989. Nucleotide sequence, organization, and nature of the protein products of the carotenoid biosynthesis gene cluster of *Rhodobacter sphaeroides*. Mol. Gen. Genet. **216:** 254–268.
2. **Batut, J., and P. Boistard.** 1994. Oxygen control in *Rhizobium*. Antonie Leeuwenhoek **66:**129–150.
3. **Cohen-Bazire, G., W. R. Sistrom, and R. Y. Stanier.** 1956. Kinetic studies of pigment synthesis by non-sulfur purple bacteria. J. Cell. Comp. Physiol. **49:**25–68.
4. **David, M., M.-L. Daveran, J. Batut, A. Dedieu, O. Domergue, J. Ghai, C. Hertig, P. Boistard, and P. Kahn.** 1988. Cascade regulation of *nif* gene expression in *Rhizobium meliloti*. Cell **54:**671–683.
5. **Davis, J., T. J. Donohue, and S. Kaplan.** 1988. Construction, characterization, and complementation of a *puf* mutant of *Rhodobacter sphaeroides*. J. Bacteriol. **170:**320–329.
6. **Eraso, J. M., and S. Kaplan.** 1994. *prrA*, a putative response regulator involved in oxygen regulation in photosynthesis gene expression in *Rhodobacter sphaeroides*. J. Bacteriol. **176:**32–43.
7. **Eraso, J. M., and S. Kaplan.** 1995. Oxygen-insensitive synthesis of the photosynthesis membranes of *Rhodobacter sphaeroides*: a mutant histidine kinase. J. Bacteriol. **177:**2695–2706.
8. **Garcia-Horsman, J. A., E. Berry, J. P. Shapleigh, J. O. Alben, and R. B. Gennis.** 1994. A novel cytochrome *c* oxidase from *Rhodobacter sphaeroides* that lacks Cu_A. Biochemistry **33:**3113–3119.
9. **Gerst, U., and S. Kaplan.** 1996. Unpublished results.
10. **Gomelsky, M., and S. Kaplan.** 1995. Genetic evidence that PpsR from *Rhodobacter sphaeroides* 2.4.1 functions as a repressor of *puc* and *bchF* expression. J. Bacteriol. **177:**1634–1637.
11. **Gong, L., and S. Kaplan.** 1996. Translational control of *puf* operon expression in *Rhodobacter sphaeroides* 2.4.1. Microbiology **142:**2057–2069.
12. **Gong, L., J. K. Lee, and S. Kaplan.** 1994. The *Q* gene of *Rhodobacter sphaeroides*: its role in *puf* operon expression and spectral complex assembly. J. Bacteriol. **176:**2946–2961.
13. **Hosler, J. P., J. Fetter, M. M. J. Tecklenberg, M. Espe, C. Lerma, and S. Ferguson-Miller.** 1992. Cytochrome aa_3 of *Rhodobacter sphaeroides* as a model for mitochondrial cytochrome *c* oxidase: purification, kinetics, proton pumping and spectral analysis. J. Biol. Chem. **267:**24264–24272.
14. **Kahn, D., M. David, O. Domergue, M.-L. Daveran, J. Ghai, P. R. Hirsch, and J. Batut.** 1989. *Rhizobium meliloti fixGHI* sequence predicts involvement of a specific cation pump in symbiotic nitrogen fixation. J. Bacteriol. **171:**929–939.
15. **Keen, N. T., S. Tamaki, D. Kobayashi, and D. Trollinger.** 1988. Improved broad-host-range plasmids for DNA cloning in gram-negative bacteria. Gene **70:**191–197.
16. **Kiley, P. J., and S. Kaplan.** 1988. Molecular genetics of photosynthetic membrane biosynthesis in *Rhodobacter sphaeroides*. Microbiol. Rev. **52:**50–69.
17. **Lang, H. P., R. J. Cogdell, S. Takaichi, and C. N. Hunter.** 1995. Complete DNA sequence, specific Tn5 insertion map, and gene assignment of the carotenoid biosynthesis pathway of *Rhodobacter sphaeroides*. J. Bacteriol. **177:**2064–2073.
18. **Lee, J. K., and S. Kaplan.** 1992. *cis*-acting regulatory elements involved in oxygen and light control of *puc* operon transcription in *Rhodobacter sphaeroides*. J. Bacteriol. **174:**1146–1157.
19. **Lee, J. K., and S. Kaplan.** 1992. Isolation and characterization of *trans*-acting mutations involved in oxygen regulation of *puc* operon transcription in *Rhodobacter sphaeroides*. J. Bacteriol. **174:**1158–1171.
20. **Lee, J. K., and S. Kaplan.** 1995. Transcriptional regulation of *puc* operon expression in *Rhodobacter sphaeroides*: Analysis of the *cis*-acting downstream regulatory sequence. J. Biol. Chem. **270:**20453–20458.
21. **Lee, J. K., P. J. Kiley, and S. Kaplan.** 1989. Posttranscriptional control of *puc* operon expression of B800-850 light-harvesting complex formation in *Rhodobacter sphaeroides*. J. Bacteriol. **171:**3391–3405.
22. **Maniatis, T., E. F. Fritsch, and J. Sambrook.** 1982. Molecular cloning: a laboratory manual. Cold Spring Harbor Laboratories, Cold Spring Harbor, N.Y.

23. **Marrs, B., and H. Gest.** 1973. Genetic mutations affecting the respiratory electron-transport system of the photosynthetic bacterium *Rhodopseudomonas capsulata*. J. Bacteriol. **114:**1045–1051.
24. **Meinhardt, S. W., P. J. Kiley, S. Kaplan, A. R. Crofts, and S. Harayama.** 1985. Characterization of light-harvesting mutants of *Rhodopseudomonas sphaeroides*. I. Measurement of the efficiency of light energy transfer from light-harvesting complexes to the reaction center. Arch. Biochem. Biophys. **236:**130–139.
25. **Neidle, E. L., and S. Kaplan.** 1992. *Rhodobacter sphaeroides rdxA*, a homolog of *Rhizobium meliloti fixG*, encodes a membrane protein which may bind cytoplasmic [4Fe-4S] clusters. J. Bacteriol. **174:**6444–6454.
26. **Neidle, E. L., and S. Kaplan.** 1993. 5-Aminolevulinic acid availability and control of spectral complex formation in HemA and HemT mutants of *Rhodobacter sphaeroides*. J. Bacteriol. **175:**2304–2313.
27. **Preisig, O., D. Anthamatten, and H. Hennecke.** 1993. Genes for a microaerobically induced oxidase complex in *Bradyrhizobium japonicum* are essential for a nitrogen-fixing endosymbiosis. Proc. Natl. Acad. Sci. USA **90:**3309–3313.
28. **Preisig, O., R. Zufferey, and H. Hennecke.** 1996. The *Bradyrhizobium japonicum fixGHIS* genes are required for the formation of the high-affinity cbb_3-type cytochrome oxidase. Arch. Microbiol. **165:**297–305.
29. **Prentki, P., and H. M. Krisch.** 1984. In vitro insertional mutagenesis with a selectable DNA fragment. Gene **29:**303–313.
30. **Sabaty, M., and S. Kaplan.** 1995. Unpublished data.
31. **Sen, P., and M. Norimoto.** 1991. Oligolabeling DNA probes to high specific activity with sequenase. Plant Mol. Biol. Rep. **9:**127–130.
32. **Shneour, E. A.** 1962. Carotenoid pigment conversion in *Rhodopseudomonas sphaeroides*. Biochim. Biophys. Acta **440:**534–540.
33. **Shneour, E. A.** 1962. The source of oxygen in *Rhodopseudomonas sphaeroides* carotenoid pigment conversion. Biochim. Biophys. Acta **65:**510–511.
34. **Siefermann-Harms, D.** 1985. Carotenoid in photosynthesis. I. Location in photosynthetic membranes and light harvesting function. Biochim. Biophys. Acta **811:**325–355.
35. **Simon, R., U. Priefer, and A. Puhler.** 1983. A broad host range mobilization system for in vivo genetic engineering: transposon mutagenesis in gram-negative bacteria. Bio/Technology **1:**37–45.
36. **Sockett, R. E., T. J. Donohue, A. R. Varga, and S. Kaplan.** 1989. Control of photosynthetic membrane assembly in *Rhodobacter sphaeroides* mediated by *puhA* and flanking sequences. J. Bacteriol. **171:**436–446.
37. **Tai, T.-N., W. A. Havelka, and S. Kaplan.** 1988. A broad-host-range vector system for cloning and translational *lacZ* fusion analysis. Plasmid **19:**175–188.
38. **Thony-Meyer, L., C. Beck, O. Preisig, and H. Hennecke.** 1994. The *ccoNOQP* gene cluster codes for a *cb*-type cytochrome oxidase that functions in aerobic respiration of *Rhodobacter capsulatus*. Mol. Microbiol. **14:**705–716.
39. **Yeliseev, A. A., J. M. Eraso, and S. Kaplan.** 1996. Differential carotenoid composition of the B875 and B800-850 photosynthetic antenna complexes in *Rhodobacter sphaeroides* 2.4.1: involvement of spheroidene and spheroidenone in adaptation to changes in light intensity and oxygen availability. J. Bacteriol. **178:**5877–5883.
40. **Yeliseev, A. A., and S. Kaplan.** 1995. A sensory transducer homologous to the mammalian peripheral-type benzodiazepine receptor regulates photosynthetic membrane complex formation in *Rhodobacter sphaeroides* 2.4.1. J. Biol. Chem. **270:**21167–21175.
41. **Yeliseev, A. A., and S. Kaplan.** Anaerobic carotenoid biosynthesis in *Rhodobacter sphaeroides* 2.4.1: H_2O is a source of oxygen for the 1-methoxy group of spheroidene but not for the 2-oxo group of spheroidenone. FEBS Lett., in press.
42. **Zeilstra-Ryalls, J. H., and S. Kaplan.** 1995. Aerobic and anaerobic regulation in *Rhodobacter sphaeroides* 2.4.1: the role of the *fnrL* gene. J. Bacteriol. **177:**6422–6431.
43. **Zeilstra-Ryalls, J. H., and S. Kaplan.** 1996. Control of *hemA* expression in *Rhodobacter sphaeroides* 2.4.1: regulation through alterations in the cellular redox state. J. Bacteriol. **178:**985–993.
44. **Zufferey, R., O. Preisig, H. Hennecke, and L. Thony-Meyer.** 1996. Assembly and function of the cytochrome cbb_3 oxidase subunits in *Bradyrhizobium japonicum*. J. Biol. Chem. **271:**9114–9119.